Acta Cryst. (1974). B30, 1318

Average and Superstructure of $K_2Mn(C_2O_4)_2.2H_2O$

BY H. SCHULZ‡

Institut für Kristallographie und Petrographie der ETH, Sonneggstrasse 5, CH-8006 *Zürich, Switzerland*

(*Received* 14 *May* 1973; *accepted* 20 *June* 1973)

Single-crystal diffraction photographs of $K_2Mn(C_2O_4)_2.2H_2O$ show superstructure as well as the main reflexions. These satellite reflexions lie on rods parallel to **b***. They cause an increase in the length of the *b* axis according to the relation *b*(super) = 4·7*b*(sub). The following results were obtained based on the main reflexions: space group $Cmc2_1$, $a = 7{\cdot}691$ (1), $b = 12{\cdot}137$ (1), $c = 10{\cdot}659$ (1) Å, $Z = 4$. The intensities of the main reflexions were collected with a diffractometer and used for the determination of the average structure ($R = 0{\cdot}084$). The main features of the average structure are layers perpendicular to **a** consisting of $C_2O_4^{2-}$ and Mn^{2+} ions. The H_2O molecules and K^+ ions occupy sites between the (C_2O_4–Mn) layers. Half the oxygen atoms of the C_2O_4 groups occupy pairs of split positions. Mean distances in the $C_2O_4^{2-}$ ions with split atoms are C–C = 1·564, C–O = 1·256 Å. The satellite reflexions are caused by transverse distortion waves. The directions and amplitudes of these distortion waves are parallel to **b** and **a** respectively. The split oxygens of the C_2O_4 ions are displaced from their averaged positions by these distortion waves. Their shifts are caused by O···H–O bonds.

1. Introduction

The crystal data given in the abstract were reported by Matthies & Schulz (1968).§ The density at room temperature is 2·32 (1) g cm^{-3}. All the water of crystallization is driven off between 120–180 °C.

The intensities of the main reflexions were measured on a Siemens off-line automatic single-crystal diffractometer with a scintillation counter, Zr-filtered Mo radiation, and a $\theta/2\theta$ scan. The crystal was spherical with a diameter of 430μ. A quarter of the reciprocal lattice was measured up to $\theta = 47°$. A reflexion intensity was set equal to zero if the net count rate (peak – background) was less than three times the standard deviation. The investigation was carried out with 1795 non-equivalent F values with $F > 0$ corrected for absorption, and weights calculated from the counting statistics.

The determination of the average structure was carried out with the X-RAY System of Stewart, Kruger Ammon, Dickinson & Hall (1972). Scattering curves were taken from *International Tables for X-ray Crystallography* (1962). The following ionic states were assumed: K^{1+}, Mn^{2+}, $O^{1/2-}$, C, H_2O.

The interpretation of the satellite reflexions (Fig. 5) follows the satellite reflexion theory (Wilson, 1962; Korekawa, 1967).

2. Average structure determination and refinement

The cell contains 4 Mn ions which must occupy the special fourfold positions 4(*a*). Their coordinates were taken from a three-dimensional Patterson synthesis: $x = 0$, $y = 0{\cdot}165$, z optional.

These coordinates were used for refinement. The initial R was 0·35. A difference synthesis showed the K ions, C_2O_4 ions and the oxygen atoms of the water molecules. With these atoms in the refinement and with isotropic and anisotropic temperature factors R dropped to 0·15 and 0·093 respectively.

The structure parameters, bond distances and angles, and the values of the thermal vibrational ellipsoids are listed in Tables 1–3. The structure is shown in Fig. 1.

The thermal vibrational ellipsoids of the atoms O(2), O(4), O(5) and O(7) have unusually large axes parallel to **a** with lengths of 0·33–0·65 Å [Fig. 2(*a*)] which can only be explained by the presence of 'split' atoms. This means that these oxygens do not occupy the refined positions (0yz), but positions ($\pm\Delta x, y, z$). Therefore, the oxygens O(2), O(4), O(5) and O(7) were not refined in the special positions 4(*a*) but in the general positions 8(*b*). The atomic parameters of the non-split atoms varied by less than one standard deviation. R dropped to 0·084. The thermal axes of the split atoms parallel to **a** are decreased [Fig. 2(*b*)] and are now comparable with those of the non-split oxygens. Structure parameters of the split atoms are also listed in Tables 1–3.

The H atoms could not be located. The final difference synthesis showed a maximum and minimum residual electron density of about ± 1 e Å^{-3}.

Observed and calculated structure factors are listed in Table 4.

3. Description of the average structure

The structure is a layer type [Fig. 1(*b*)] consisting of layers of C_2O_4 and Mn ions, which occupy sites within the mirror planes intersecting **a** at $x = 0{\cdot}0$ and $x = 0{\cdot}5$. The K ions and H_2O molecules are arranged between the (C_2O_4–Mn) layers.

‡ Present address: Institut für Kristallographie, J.W. Goethe Universität, Senckenberganlage 30, D-6 Frankfurt a. M., Germany.

§ In the paper of Matthies & Schulz the number of formula units per elementary cell must be corrected to $Z = 4$.

Table 1. *Structure parameters*

	Equi-point	x	y	z	U (Å²)	U_{11} (Å²)	U_{22} (Å²)	U_{33} (Å²)	U_{12} (Å²)	U_{13} (Å²)	U_{23} (Å²)
Mn	4(*a*)	0·0	0·1765 (1)	0·5	0·0197 (3)	0·0274 (7)	0·0168 (5)	0·0187 (5)	0·0	0·0	−0·001 (6)
K	8(*b*)	0·2487 (4)	0·0957 (2)	0·2016 (3)	0·0381 (6)	0·038 (1)	0·052 (1)	0·034 (1)	−0·003 (1)	0·015 (1)	0·002 (1)
O(1)	4(*a*)	0·0	0·2464 (8)	0·305 (1)	0·024 (2)	0·048 (6)	0·011 (3)	0·017 (4)	0·0	0·0	−0·001 (3)
O(2)	4(*a*)	0·0	0·405 (1)	0·205 (2)	0·068 (8)	0·220 (4)	0·020 (5)	0·018 (5)	0·0	0·0	0·005 (5)
O(3)	4(*a*)	0·0	0·3567 (7)	0·5241 (9)	0·022 (2)	0·035 (5)	0·013 (3)	0·018 (4)	0·0	0·0	−0·001 (2)
O(4)	4(*a*)	0·0	0·510 (1)	0·409 (2)	0·086 (11)	0·380 (6)	0·013 (4)	0·025 (6)	0·0	0·0	−0·001 (4)
O(5)	4(*a*)	0·5	0·2539 (9)	0·297 (1)	0·035 (4)	0·110 (2)	0·012 (4)	0·020 (4)	0·0	0·0	−0·003 (3)
O(6)	4(*a*)	0·5	0·4063 (9)	0·1810 (9)	0·022 (2)	0·040 (5)	0·020 (3)	0·009 (3)	0·0	0·0	−0·00 (3)
O(7)	4(*a*)	0·5	0·378 (1)	0·505 (2)	0·052 (5)	0·180 (2)	0·018 (4)	0·013 (4)	0·0	0·0	−0·003 (5)
O(8)	4(*a*)	0·5	0·5288 (8)	0·388 (1)	0·024 (2)	0·053 (7)	0·012 (3)	0·018 (4)	0·0	0·0	−0·003 (3)
H_2O	8(*b*)	0·280 (1)	0·1869 (7)	0·514 (1)	0·025 (2)	0·020 (2)	0·036 (3)	0·034 (5)	−0·001 (2)	0·003 (3)	0·006 (3)
C(1)	4(*a*)	0·0	0·348 (1)	0·297 (1)	0·042 (4)	0·070 (1)	0·026 (5)	0·023 (5)	0·0	0·0	0·002 (4)
C(2)	4(*a*)	0·0	0·413 (1)	0·423 (1)	0·045 (5)	0·080 (1)	0·020 (5)	0·030 (6)	0·0	0·0	−0·009 (4)
C(3)	4(*a*)	0·0	0·355 (1)	0·281 (1)	0·027 (3)	0·029 (5)	0·023 (4)	0·022 (4)	0·0	0·0	−0·007 (4)
C(4)	4(*a*)	0·0	0·428 (1)	0·404 (1)	0·024 (3)	0·034 (5)	0·019 (4)	0·021 (4)	0·0	0·0	−0·002 (3)
Split atoms											
O(2)	8(*b*)	0·051 (2)	0·405 (1)	0·206 (1)		0·048 (8)	0·020 (4)	0·018 (5)	−0·002 (5)	0·010 (5)	0·005 (4)
O(4)	8(*b*)	0·060 (3)	0·509 (1)	0·410 (2)		0·086 (13)	0·015 (4)	0·027 (6)	−0·022 (6)	0·013 (7)	−0·003 (4)
O(5)	8(*b*)	0·531 (2)	0·254 (1)	0·297 (1)		0·034 (11)	0·013 (3)	0·020 (4)	0·004 (4)	0·002 (6)	−0·003 (3)
O(7)	8(*b*)	0·541 (2)	0·378 (1)	0·505 (2)		0·046 (8)	0·018 (3)	0·013 (3)	0·004 (4)	−0·009 (5)	−0·003 (4)

Table 2. *Bond distances and angles*

Average structure Bond distances and angles of the model without split atoms		Superstructure Essential bond distances and angles which differ from those in the average structure	
C(1)–C(2)	1·552 (18) Å		
C(1)–O(1)	1·237 (17)		
C(1)–O(2)	1·203 (17)	1·261 (17) Å	
C(2)–O(3)	1·280 (17)		
C(2)–O(4)	1·195 (19)	1·278 (18)	
O(1)–C(1)–O(2)	129 (1)°	127 (1)°	
O(1)–C(1)–C(2)	117 (1)		
O(2)–C(1)–C(2)	114 (1)	113 (1)	
O(3)–C(2)–O(4)	130 (1)	126 (1)	
O(3)–C(2)–C(1)	117 (1)		
O(4)–C(2)–C(1)	113 (1)	112 (1)	
C(3)–C(4)	1·578 (19) Å		
C(3)–O(5)	1·239 (13)	1·259 (13) Å	
C(3)–O(6)	1·233 (15)		
C(4)–O(7)	1·230 (20)	1·268 (20)	
C(4)–O(8)	1·241 (16)		
O(5)–C(3)–O(6)	128 (1)°	127 (1)°	
O(5)–C(3)–C(4)	116 (1)	115 (1)	
O(6)–C(3)–C(4)	116 (1)		
O(7)–C(4)–O(8)	127 (2)	126 (1)	
O(7)–C(4)–C(3)	117 (1)	116 (1)	
O(8)–C(4)–C(3)	116 (1)		
Mn–O(8)	2·15 (1) Å		
Mn–H_2O	2·166 (1)		
Mn–H_2O	2·166 (1)		
Mn–O(6)	2·18 (1)		
Mn–O(3)	2·20 (1)		
Mn–O(1)	2·25 (1)		
O(1)–Mn–O(3)	74·5 (4)°		
O(1)–Mn–O(6)	174·7 (7)		
O(1)–Mn–O(8)	78·5 (4)		
O(1)–Mn–H_2O	92·5 (4)		
O(3)–Mn–O(6)	110·8 (4)		
O(3)–Mn–O(8)	153·0 (5)		
O(3)–Mn–H_2O	86·2 (6)		
O(6)–Mn–O(8)	96·2 (4)		
O(6)–Mn–H_2O	87·9 (4)		
O(8)–Mn–H_2O	95·0 (4)		
H_2O–Mn–H_2O	169·5 (6)		
		1st co-ordination	2nd co-ordination
K–O(3)	2·766 (8) Å		
K–O(7)	2·856 (9)	3·080 (8) Å	2·653 (9) Å
K–O(1)	2·866 (10)		
K–O(8)	2·874 (9)		
K–O(5)	2·910 (8)	2·760 (8)	3·071 (7)
K–O(6)	2·999 (9)		
K–O(2)	3·016 (9)	2·778 (13)	3·280 (14)
K–O(4)	3·106 (15)	3·448 (16)	2·846 (17)
O(1)–K–O(2)	155·9 (4)°		
O(1)–K–O(3)	126·6 (3)		
O(1)–K–O(4)	110·8 (3)		
O(1)–K–O(5)	83·5 (3)		
O(1)–K–O(6)	95·3 (3)		
O(1)–K–O(7)	76·3 (3)		
O(1)–K–O(8)	58·0 (3)		
O(2)–K–O(3)	73·8 (3)		
O(2)–K–O(4)	48·5 (3)		
O(2)–K–O(5)	94·4 (3)		
O(2)–K–O(6)	79·7 (3)		
O(2)–K–O(7)	121·6 (3)		
O(2)–K–O(8)	101·6 (3)		

Table 2 (*cont.*)

O(3)–K–O(4)	96·9 (3)°	
O(3)–K–O(5)	68·8 (3)	
O(3)–K–O(6)	123·8 (3)	
O(3)–K–O(7)	86·7 (3)	
O(3)–K–O(8)	175·4 (4)	
O(4)–K–O(5)	63·7 (3)	
O(4)–K–O(6)	101·2 (3)	
O(4)–K–O(7)	167·0 (3)	
O(4)–K–O(8)	80·2 (3)	
O(5)–K–O(6)	162·8 (4)	
O(5)–K–O(7)	128·9 (3)	
O(5)–K–O(8)	112·7 (3)	
O(6)–K–O(7)	66·8 (3)	
O(6)–K–O(8)	53·8 (3)	
O(7)–K–O(8)	95·4 (3)	
H_2O–O(2)	2·87 (2) Å	2·66 (2) Å
H_2O–O(7)	2·87 (1)	2·70 (2)
H_2O–O(4)	2·95 (2)	2·70 (2)
H_2O–O(5)	2·98 (1)	2·85 (2)
H_2O–O(3)	2·99 (1)	
H_2O–O(6)	3·02 (1)	
H_2O–O(8)	3·18 (1)	
H_2O–O(1)	3·19 (2)	
O(1)–H_2O–O(2)	169·4 (5)	
O(1)–H_2O–O(3)	51·6 (3)	
O(1)–H_2O–O(4)	106·4 (6)	
O(1)–H_2O–O(5)	77·1 (4)	
O(1)–H_2O–O(6)	90·8 (3)	
O(1)–H_2O–O(7)	101·0 (5)	
O(1)–H_2O–O(8)	51·8 (3)	
O(2)–H_2O–O(3)	132·0 (6)	
O(2)–H_2O–O(4)	69·7 (5)	
O(2)–H_2O–O(5)	108·9 (2)	119·6 (4)°
O(2)–H_2O–O(6)	81·8 (4)	
O(2)–H_2O–O(7)	89·6 (3)	
O(2)–H_2O–O(8)	117·7 (5)	
O(3)–H_2O–O(4)	158·0 (6)	
O(3)–H_2O–O(5)	104·3 (5)	
O(3)–H_2O–O(6)	73·8 (3)	
O(3)–H_2O–O(7)	82·5 (4)	
O(3)–H_2O–O(8)	86·6 (2)	
O(4)–H_2O–O(5)	64·9 (4)	
O(4)–H_2O–O(6)	111·3 (5)	
O(4)–H_2O–O(7)	103·6 (3)	116·4 (3)
O(4)–H_2O–O(8)	77·8 (3)	
O(5)–H_2O–O(6)	165·1 (5)	
O(5)–H_2O–O(7)	54·4 (4)	
O(5)–H_2O–O(8)	102·7 (5)	
O(6)–H_2O–O(7)	138·1 (6)	
O(6)–H_2O–O(8)	62·6 (3)	
O(7)–H_2O–O(8)	150·4 (6)	

The Mn atoms are coordinated octahedrally (Fig. 3). The base of this octahedron is formed by the non-split oxygens of the C_2O_4 groups and the apices of the octahedron are formed by the water molecules.

The K ions are coordinated by 8 oxygen atoms in the form of a distorted cube (Fig. 4).

4. Features of the satellite reflexion pattern

In Fig. 5 Weissenberg photographs of the (*hkl*) layers with $h=0,1,2$ are shown. In Fig. 6 the diffraction pat-

Table 3. *Principal thermal axes and their directions*

	Length of main axes (Å)	Angle with *a* axis (°)	Angle with $-b$ axis (°)	Angle with $-c$ axis (°)
Mn	0·130 (2)	90	175 (42)	95 (42)
	0·133 (2)	90	95 (42)	5 (42)
	0·167 (2)	0	90	90
K	0·162 (4)	41·9 (3)	115 (5)	59·0 (2)
	0·189 (3)	69·9 (4)	25 (5)	75·6 (3)
	0·245 (3)	55·1 (2)	90 (2)	145·1 (2)
O(1)	0·10 (2)	90	170 (44)	100 (44)
	0·13 (2)	90	100 (44)	10 (44)
	0·22 (3)	0	90	90
O(2)	0·12 (2)	90	49 (24)	139 (24)
	0·15 (1)	90	41 (24)	49 (24)
	0·50 (2)	0	90	90
O(3)	0·11 (2)	90	169 (36)	101 (36)
	0·13 (1)	90	101 (36)	11 (36)
	0·19 (1)	0	90	90
O(4)	0·11 (2)	90	167 (35)	77 (35)
	0·14 (1)	90	77 (35)	13 (35)
	0·65 (2)	0	90	90
O(5)	0·11 (2)	90	156 (19)	114 (19)
	0·14 (1)	90	114 (19)	24 (19)
	0·33 (1)	0	90	90
O(6)	0·10 (2)	90	93 (19)	117 (19)
	0·14 (1)	90	3 (19)	93 (19)
	0·20 (1)	0	90	90
O(7)	0·10 (2)	90	113 (18)	157 (18)
	0·14 (1)	90	23 (18)	113 (18)
	0·43 (1)	0	90	90
O(8)	0·10 (2)	90	158 (23)	112 (23)
	0·14 (2)	90	112 (23)	22 (23)
	0·23 (1)	0	90	90
H_2O	0·14 (3)	20 (23)	99 (13)	73 (19)
	0·17 (1)	109 (23)	125 (16)	42 (18)
	0·20 (1)	87 (3)	143 (16)	127 (16)
C(1)	0·14 (2)	90	73 (25)	163 (25)
	0·16 (1)	90	17 (25)	73 (25)
	0·26 (1)	0	90	90
C(2)	0·12 (2)	90	148 (11)	122 (11)
	0·18 (1)	90	122 (11)	32 (11)
	0·28 (7)	0	90	90
C(3)	0·13 (1)	90	133 (10)	137 (10)
	0·17 (1)	90	43 (10)	133 (10)
	0·17 (1)	0	90	90
C(4)	0·13 (2)	90	142 (51)	128 (51)
	0·15 (2)	90	128 (51)	38 (51)
	0·18 (2)	0	90	90
Split atoms				
O(2)	0·11 (2)	104 (7)	59 (15)	145 (13)
	0·15 (1)	83 (8)	32 (15)	60 (15)
	0·23 (2)	15 (8)	89 (7)	106 (9)
O(4)	0·09 (2)	74 (4)	164 (5)	89 (16)
	0·15 (1)	80 (6)	86 (16)	11 (5)
	0·31 (1)	19 (3)	74 (3)	100 (4)
O(5)	0·10 (1)	100 (3)	156 (14)	112 (16)
	0·14 (1)	89 (4)	112 (15)	22 (15)
	0·19 (2)	10 (3)	99 (3)	95 (2)
O(7)	0·10 (2)	79 (4)	102 (21)	164 (13)
	0·13 (1)	79 (6)	15 (18)	99 (21)
	0·22 (1)	16 (3)	99 (2)	77 (2)

tern is shown in a schematic way. The main features of the satellite diffraction pattern are:

1. The satellite reflexions are only observable in layers with $h \neq 0$. (The diffuse streaks in Fig. 5(*a*) are caused by the grinding of the crystal sphere.)

2. The satellite reflexions lie on rods parallel to **b***. Only **b** is enlarged by the satellite reflexions.

3. The satellite reflexions are arranged around the extinct main reflexions with $h+k=2n+1$.

4. b of the supercell [b(super)] can be calculated from the distance d_s^* between the reflexions of a satellite pair: $b^*(\text{super}) = d_s^*/2$ Å^{-1} and therefore $b(\text{super}) = 2/d_s^*$ Å. From 10 measurements it follows that $b(\text{super}) = 57{\cdot}5$ (7) Å. The ratio of $b(\text{super}):b(\text{sub}) =$

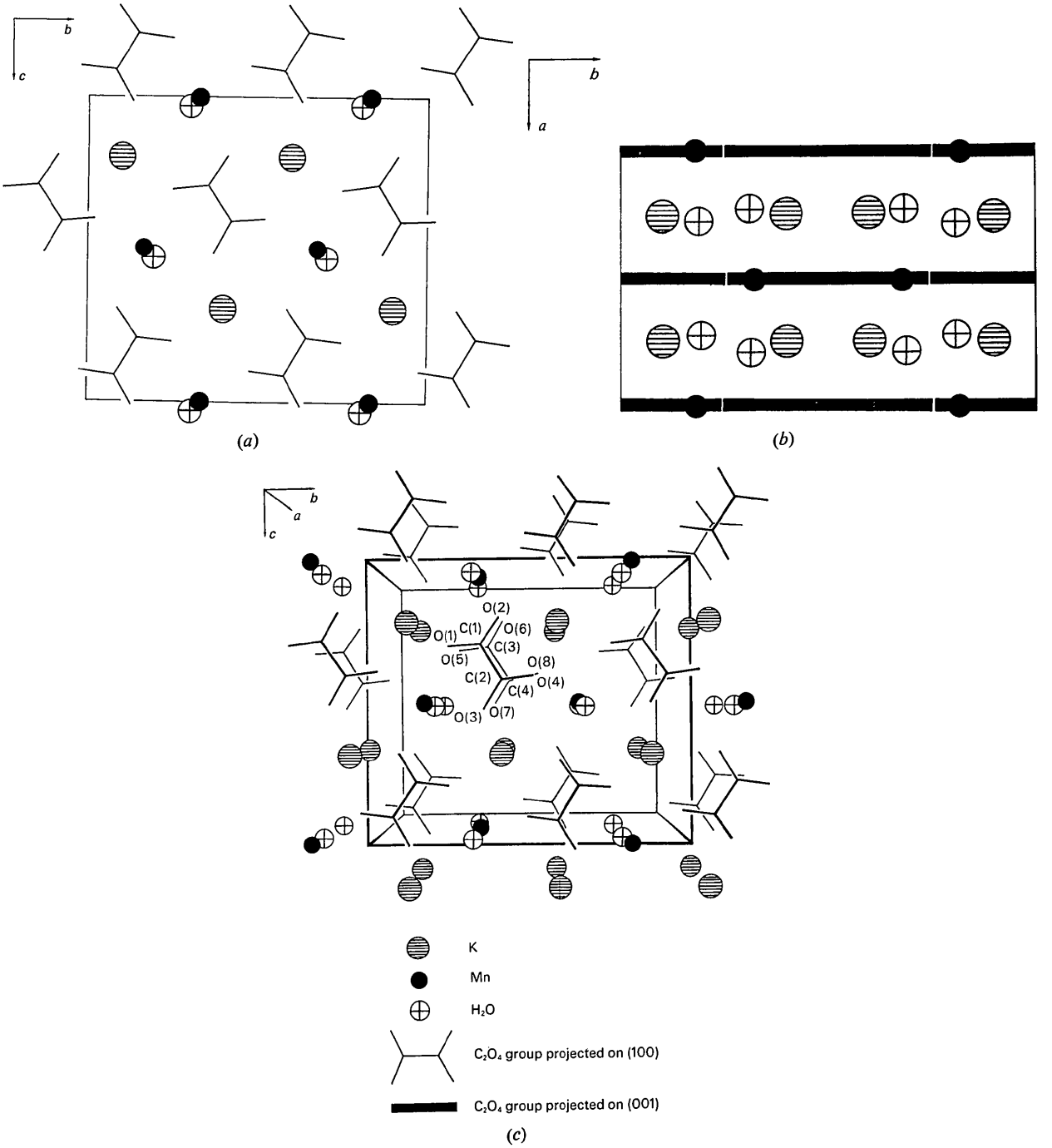

Fig. 1. Structure projections. Schematic projection on (*a*) (100), (*b*) (001). (*c*) Central projection on (100). The designations C(1)–C(4) and O(1)–O(8) refer to the corresponding atoms listed in Table 1.

57·5 (7):12·137 (1)=4·74 (6) is significantly different from an integer.

5. Only one distance d_S^* is observable, thus only satellites of one order are observable.

6. More qualitative observations were made as follows:

(*a*) The intensities of the satellites are weak compared with the intensities of the main reflexions.
(*b*) The satellite reflexions are diffuse.
(*c*) No relations between intensities of main reflexions and satellite reflexions are observable.

5. Elements of the satellite reflexion theory

Only so-called transverse distortion waves (Dehlinger, 1927) and phase shifts of distortion waves (Korekawa, 1967) are used in the following. The corresponding calculations are given in the Appendix, and the results of these calculations are described in this section.

Fig. 7(*a*) and (*b*) shows an undistorted *C* face-centred structure and the corresponding reciprocal lattice. The atoms occupy so-called 'ideal' sites. In Fig. 7(*c*) the atoms are moved away from their ideal sites to their real sites by a sinusoidal distortion wave. The transverse distortion wave is characterized by

(*a*) its direction,
(*b*) its wavelength,
(*c*) its amplitude *A*,
(*d*) direction of its amplitude.

Thus Fig. 7(*c*) shows

(*a*) the direction of the distortion is parallel to **b**,
(*b*) its wavelength is 8 times larger than *b*(sub),

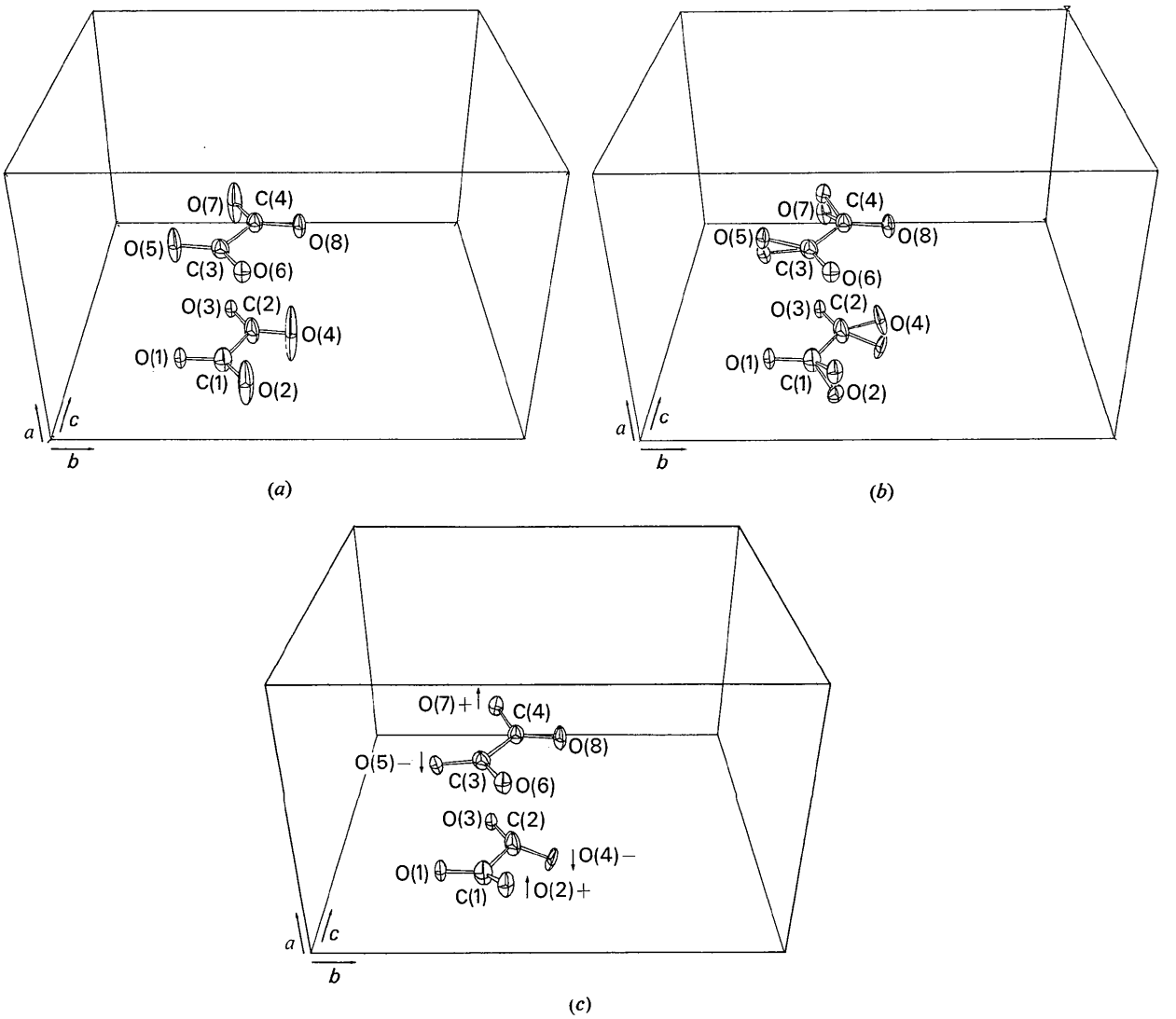

Fig. 2. Atomic arrangement and anisotropic temperature factors of the symmetry-independent oxalate ions in relation to the axes of the elementary cell of the average structure. The thermal vibrational ellipsoids are scaled to include 50% probability. Average structure (*a*) without split atoms, (*b*) with split atoms. (*c*) Superstructure (atomic arrangement in subcells I and II of Fig. 10*b*). The designations C(1)–C(4) and O(1)–O(8) refer to the corresponding atoms listed in Table 1.

(*c*) the amplitude A is about $\frac{1}{5}$ of a,
(*d*) the direction of the amplitude is parallel to **a**.
Fig. 7(*d*) shows the corresponding reciprocal lattice. The observable 'main reflexions' $(h+k=2n)$ are accompanied by satellite reflexions.

In our case the intensities of the main and satellite reflexions I_M and I_S are a function of the product Ah.

$$I_M \sim J_0^2(2\pi Ah)$$
$$I_S \sim J_1^2(2\pi Ah')$$

h' is the h value of the satellite reflexions, which can be written as $h' = h \pm \Delta h$

J_0 and J_1 are Bessel functions of order 0 and 1 respectively.

The J_0^2 and J_1^2 are shown in Fig. 8 as a function of $2\pi Ah$. An important fact is that $I_S = 0$ if $2\pi Ah = 0$, that is $h = 0$ [see Fig. 7(*d*)]. This means that satellite reflexions are not observable in the $(0kl)$ layer if the direction of the amplitude A is parallel to **a**.

In Fig. 7(*e*) both atoms of each elementary cell are again influenced by the same distortion waves, but the two distortion waves running through an elementary cell have a phase shift of π relative to each other. This means that if the atom at the origin of an elementary

Table 4. *Observed and calculated structure factors*

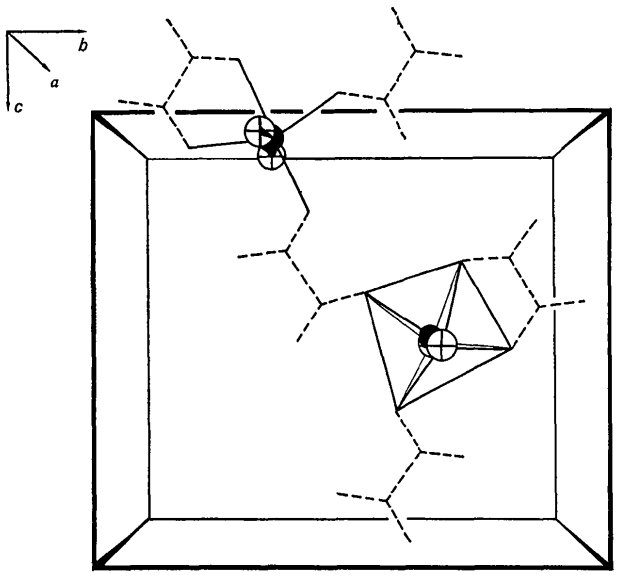

Fig. 3. Coordination polyhedron and bonds of the Mn atoms.

cell is displaced in the positive direction of **a** by $+\Delta a$ the atom at the centre of this elementary cell is shifted in the opposite direction by $-\Delta a$ and *vice versa*. The influence of this phase shift on the diffraction pattern is shown in Fig. 7(*f*). The satellite reflexions are now arranged around the extinct main reflexions with $h+k=2n+1$. All other features of the diffraction pattern agree with those of Fig. 7(*d*).

6. Distorted structure elements of the oxalate structure

A comparison of Figs. 6 and 7(*f*) shows that transverse distortion waves are present in the oxalate structure. They are of the same sort as in Fig. 7(*e*).

In contrast to Fig. 7(*f*), however, a relation between the intensities of main and superstructure reflexions is not observable. Furthermore, the intensities of the satellite reflexions are weak compared with the main reflexions (§ 4, Point 6). Therefore one can assume that only parts of the structure are distorted and that their scattering power is weak compared with the scattering power of the whole structure. It is probable that the four split oxygens produce the intensities of the satellite reflexions. This assumption is supported by the direction of the lines connecting the split atom positions, which is parallel to **a** [Fig. 2(*b*)] and thereby parallel to the amplitude of the observed distortion waves.

7. Influence of O···H–O bonds on the superstructure

The Mn atoms occupy sites within the mirror planes. They are coordinated by four oxygens and two water molecules in the form of an octahedron. If all Mn atoms were shifted parallel to **a** by **a**/2 they would again occupy sites within a mirror plane and would again be coordinated by four oxygen atoms and two water molecules in the form of an octahedron. These two sorts of octahedra, occupied and unoccupied, form the chains shown in Fig. 9. All oxygen atoms and all water molecules participate in the construction of these chains. Each elementary cell contains four occupied and four unoccupied octahedra. Four chains run through each elementary cell. It is now an important fact that the non-split oxygens form the bases of the occupied octahedra, whereas the bases of the unoccupied octahedra are formed only by the split oxygens (marked by arrows in Fig. 9).

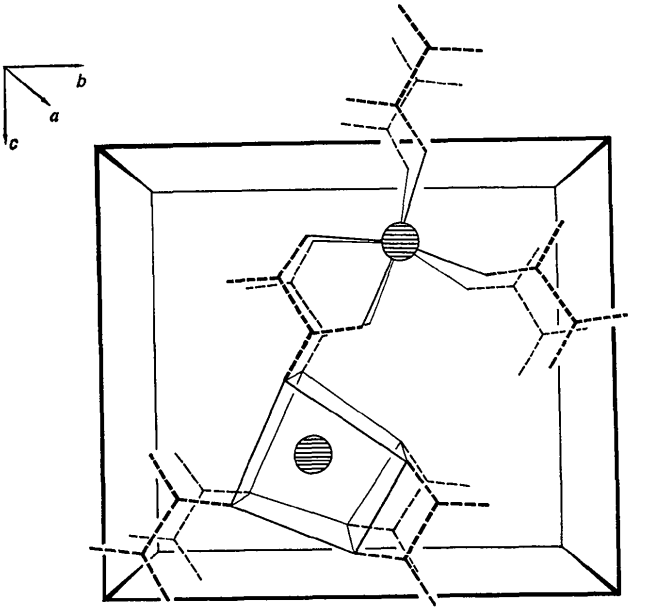

Fig. 4. Coordination polyhedron and bonds of the K atoms.

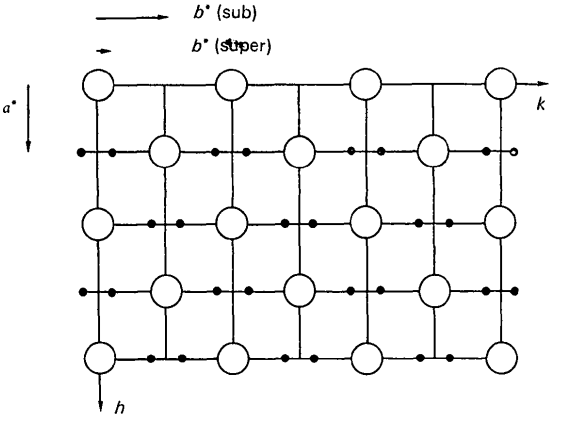

Fig. 6. Schematic presentation of the diffraction pattern of $K_2Mn(C_2O_4)_2\ 2H_2O$ neglecting the influence of the structure factor, scattering power and thermal motion on the diffracted intensities. ○ main reflexions, ● satellite reflexions.

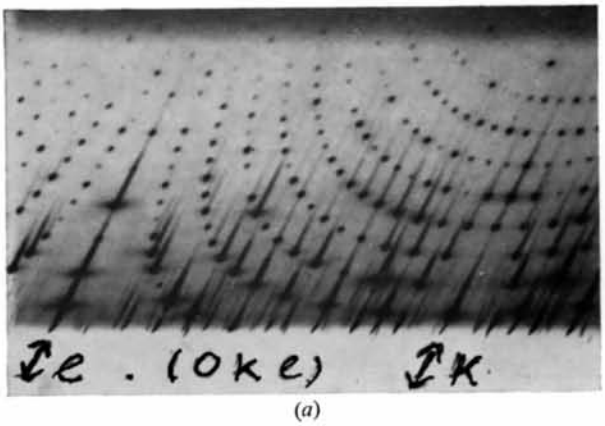

(*a*)

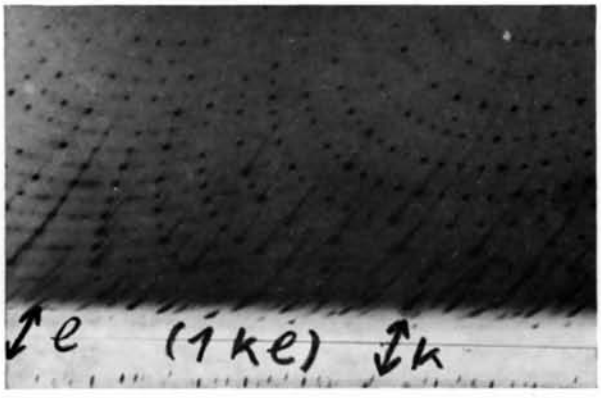

(*b*)

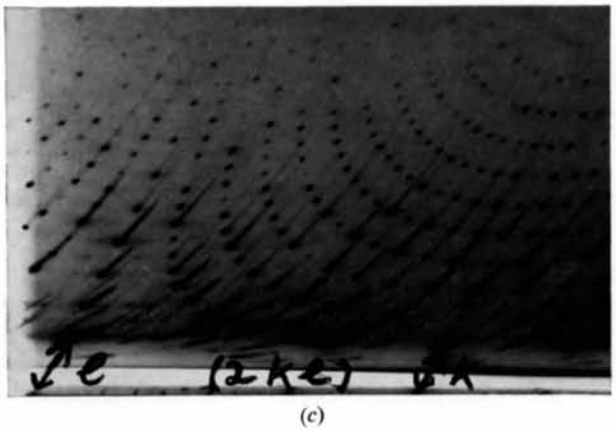

(*c*)

Fig. 5. Weissenberg photographs with filtered Mo radiation.
(*a*) 0*kl* layer: no satellite reflexion observable.
(*b*) 1*kl* layer: diffuse satellite reflexions observable on rods parallel to **b***.
(*c*) 2*kl* layer: diffuse satellite reflexions observable on rods parallel to **b***.

[*To face p.* 1324

The hydrogen atoms have not been considered up to now. As Fig. 9 shows, all water molecules are surrounded by 8 oxygen atoms. Therefore each of these oxygens may be used as a bonding partner for the $O\text{–}H_2O\text{–}O$ bonds. This leads to 8 $O\text{–}H_2O\text{–}O$ distances and 28 $O\text{–}H_2O\text{–}O$ angles (Table 2). Only two of these 28 arrangements are in agreement with the known distances and bond angles of $O\cdots H\text{–}O\text{–}H\cdots O$.

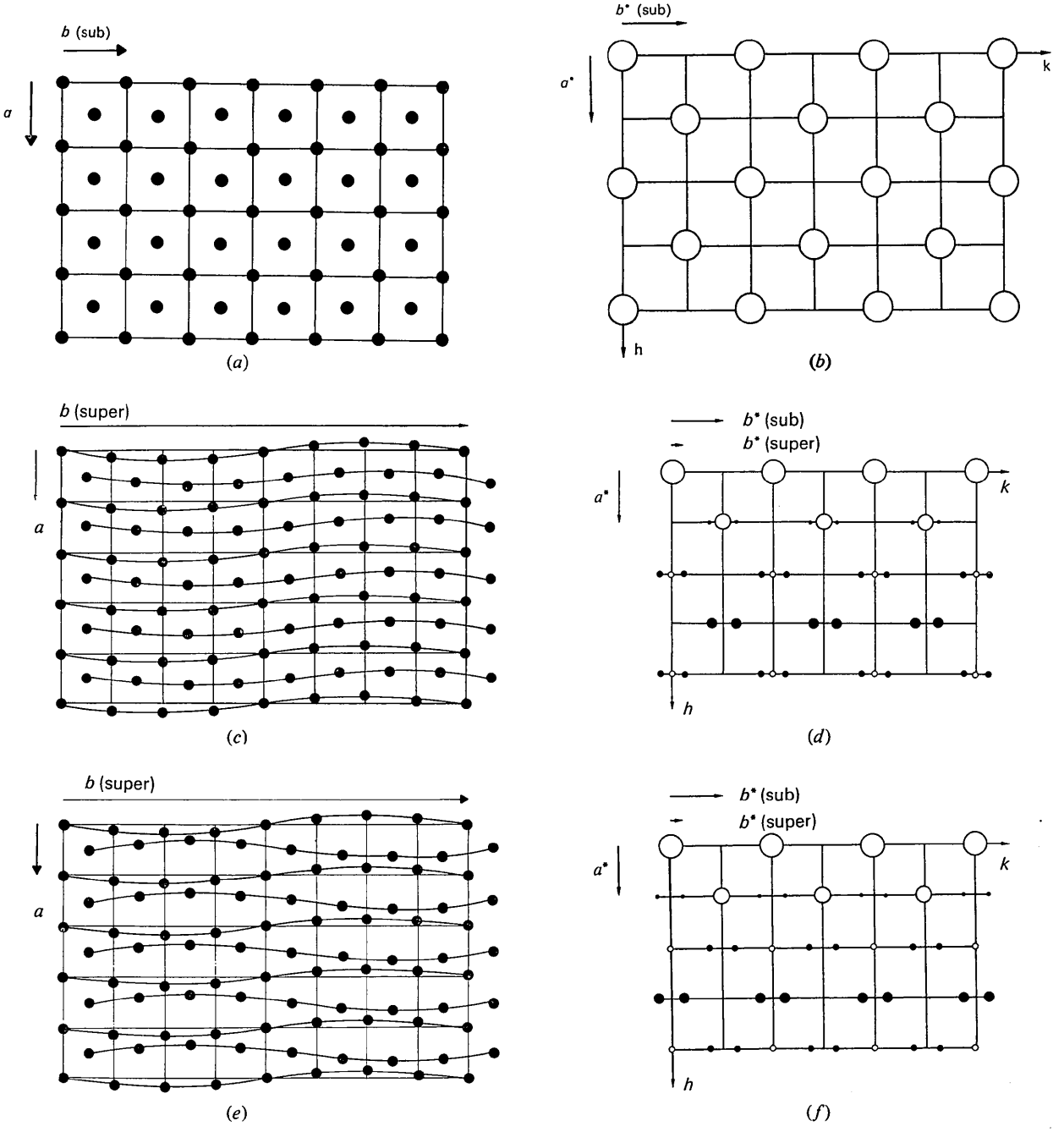

Fig. 7. Relation between distorted crystal structures and diffraction patterns. In the diffraction patterns, (*b*), (*d*), (*f*), the influence of scattering power and thermal motion on the diffracted intensities is neglected. (*a*) Undistorted *C* face-centred structure; (*b*) diffraction pattern of structure *a*; (*c*) *C* face-centred structure influenced by sinusoidal distortion waves. The phase shifts of the distortion waves running through a subcell equal zero; (*d*) diffraction pattern of structure *c*; (*e*) *C* face-centred structure influenced by sinusoidal distortion waves. The phase shifts of the distortion waves running through a subcell equal π; (*f*) diffraction pattern of structure *e*; ● atoms of the same sort, ○ ○ main reflexions of different intensities, ● ● satellite reflexions of different intensities. The intensities are proportional to the diameters of the open and blocked circles.

These combinations are:

1. H_2O–O(2) = 2·87 Å
   H_2O–O(5) = 2·98 Å
   O(2)–H_2O–O(5) = 108·9°
2. H_2O–O(4) = 2·95 Å
   H_2O–O(7) = 2·87 Å
   O(4)–H_2O–O(7) = 103·6°

It follows that only the split oxygens O(2), O(4), O(5) and O(7) are included in O···H–O bonds. These four oxygen atoms form O···H–O bonds with the two water molecules at the tops of the unoccupied octahedra (Fig. 9). Only two possibilities exist for arranging these four O···H–O bonds. They are shown in Fig. 10(*a*) and are designated *A* and *B*. The superstructure is generated by an ordered distribution of the *A* and *B* arrangements. This can be demonstrated by the superstructure model of Fig. 10(*b*). Each subcell of Fig. 10(*b*) contains only the atoms forming unoccupied octahedra. The unoccupied octahedra of Fig. 9 are replaced in Fig. 10(*b*) by configurations *A* or *B*. For clarity, only the O···H–O bonds of configurations *A* and *B* are drawn. The atomic positions in Fig. 10(*b*) are the average positions and therefore exactly *C* face-centred.

The superstructure model of Fig. 10(*b*) is based on the following assumptions:

(1) The superstructure cell consists of four subcells which are situated behind each other in the **b** direction. Therefore *b*(super) = 4*b*(sub).

(2) If in a subcell one of the unoccupied octahedra is replaced by configuration *A*, then the *C* face-centred one is replaced by configuration *B*. For example, in subcell I of Fig. 10(*b*) configurations *A* and *B* are present in the lower left and upper right corners respectively.

(3) The arrangement of the subcell I is repeated in subcell II and reversed in subcells III and IV.

(4) The positions of the oxygen atoms in the superstructure depend on the position of the H_2O molecule to which they are bonded. The oxygens are displaced from their average positions parallel to **a** as shown by the arrows in Fig. 10(*b*). The O···H–O bonds are thereby shorter in the superstructure than in the average structure.

The superstructure model of Fig. 10(*b*) meets nearly all the conditions and features derived from the average structure and the satellite pattern:

(*a*) By superposition of the four subcells of Fig. 10(*b*) the average structure is derived. The H_2O molecules occupy equal positions in each subcell. Consequently the superimposed water molecules do not occupy split positions in the average structure. The same is true for the K, Mn and the O(1), O(3), O(6) and O(8) atoms, which have therefore already been excluded from Fig. 10(*b*). Only the superimposed O(2), O(4), O(5) and O(7) atoms form split atom pairs. Their split directions are parallel to **a**, and this agrees with the experimental observations.

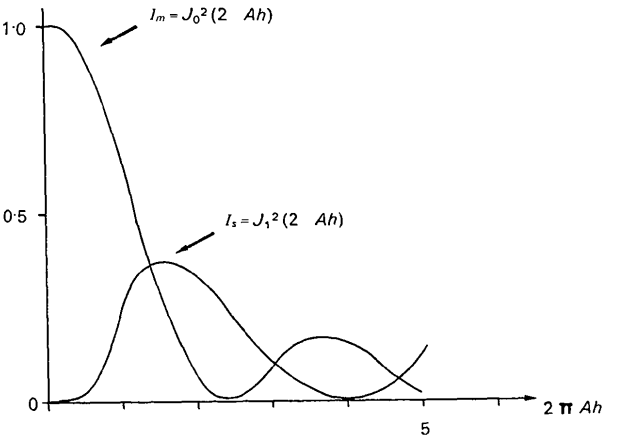

Fig. 8. Squares of the Bessel functions J_0^2 and J_1^2 as a function of $2\pi Ah$.

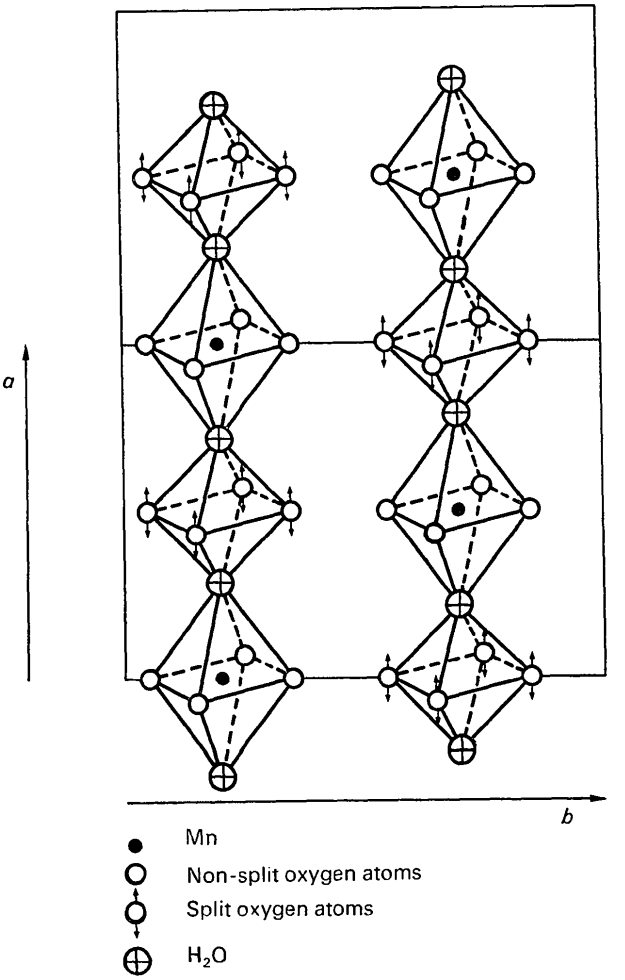

Fig. 9. Octahedra chains. Four of these chains run through each subcell. The two chains in the figure are related to each other by the *C* face-centring. The *z* coordinates of Mn ions and H_2O are about 0·5.

(*b*) Only the split oxygens contribute to the satellite reflexions. Their scattering power is small compared with that of the whole structure. Therefore the intensities of the satellite reflexions must be weak compared with the main reflexions, which is in agreement with the observed diffraction pattern.

(*c*) As shown in § 6 the general features of the proposed superstructure model [Fig. 10(*b*)] and the superstructure of Fig. 7(*e*) must agree. From Fig. 10(*b*) it follows:

(i) *Distortion waves*

The distortion function can be read from Fig. 10(*b*) by considering the same oxygen average position in the four subcells. The corresponding oxygen shifts (marked by the arrows) follow a sine curve. This is shown in Fig. 11, in which the displacements for one oxygen position are drawn.

(ii) *Phase shift of the distortion waves*

C face-centred oxygen positions of a subcell are influenced by the same distortion waves but these two waves have a phase shift of π. This can be read from the corresponding oxygen shifts. *C* face-centred oxygens in each subcell are shifted in *opposite* directions by the *same amount*.

(iii) *Direction of the distortion waves*

The direction of the distortion waves is parallel to **b**. Only **b** is enlarged such that $b(\text{super}) = 4b(\text{sub})$.

(iv) *Directions and magnitudes of the amplitudes of the distortion waves*

The displacements of the oxygen atoms from their average positions are parallel to **a**. The magnitudes of the distortion amplitudes are equal for all oxygens in Fig. 10(*b*). This is not required by the calculations in the Appendix. Only those oxygen atoms which occupy the same atomic position in the average structure must have equal displacements.

As required in § 6, the general features (i)–(iv) agree with those of Fig. 7(*e*).

The space-group symmetry of the average structure $Cmc2_1$ is lowered by the superstructure. The calculations in the Appendix prove that the remaining symmetry of each subcell of a supercell is $P1c1$. By application of $P1c1$ to each subcell of Fig. 10(*b*) the complete superstructure is generated. This superstructure indicates which water molecule and oxygen atoms are bonded together, and from this result the real arrangement of the C_2O_4 ions within the superstructure can be read. Tables 5 and 6 list the coordinates of O–H_2O–O bonds and C_2O_4 ions within the super-

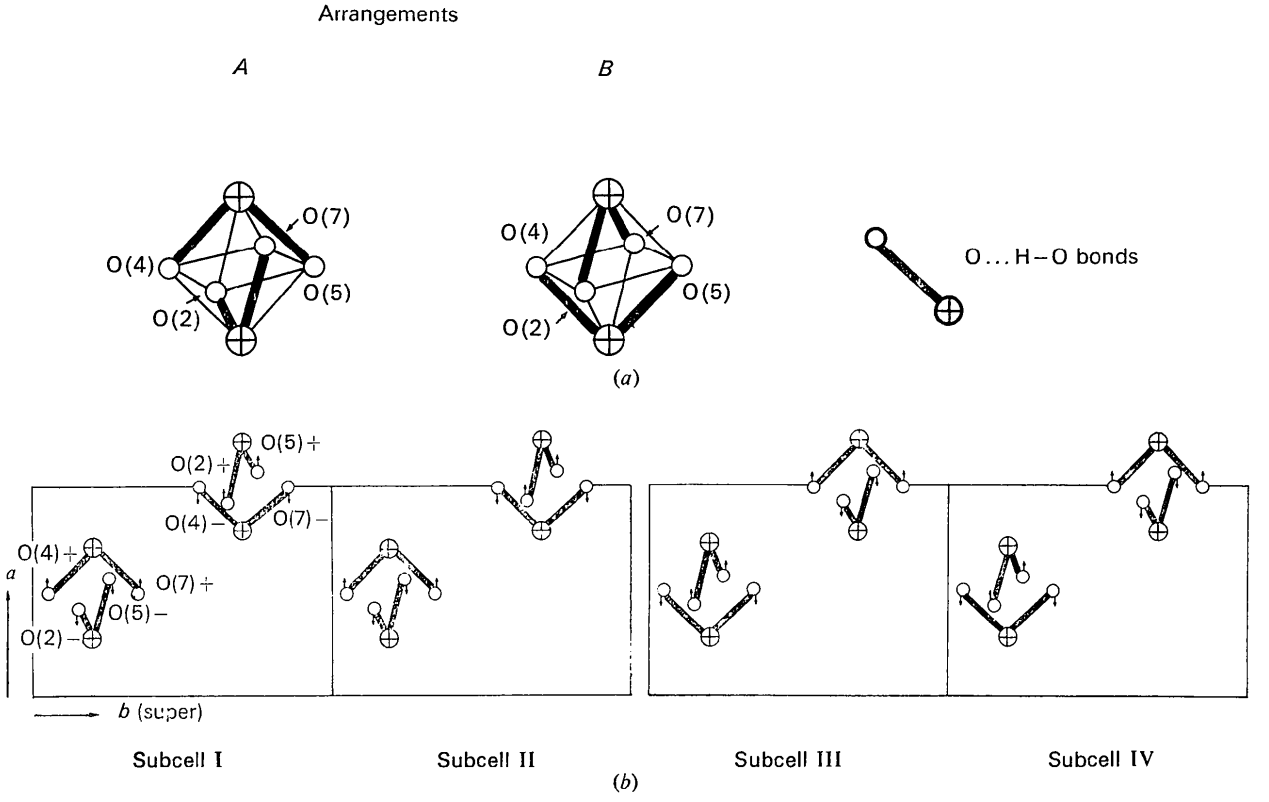

Fig. 10. Proposed superstructure model. The *x* coordinates of H_2O are about 0·5. Symbols as in Fig. 9. (*a*) The two possible arrangements of O–H_2O–O bonds. (*b*) Ordered distribution of O–H_2O–O bonds and related displacements of the oxygens. The deviations of the oxygens from their average position are shown by arrows. The tops of these arrows represent the oxygen position within the superstructure.

cell. These coordinates are derived in the following way:

1. The occupied oxygen split positions are read from Fig. 10(*b*).

2. The coordinates of the split positions are taken from the structure refinement with split atoms (Table 1).

3. The atomic coordinates of the non-split atoms have equal values in each subcell and are also taken from Table 1. They are only included in Tables 5 and 6 in order to give a convenient survey of the real atomic positions within the supercell.

Two independent C_2O_4 groups of subcells I and II are shown in Fig. 2(*c*).

Table 5. $O–H_2O–O$ *bonds of the superstructure*

The atomic positions of the Table are taken from subcell I of Fig. 6(*b*). The coordinates are related to axes of the subcell. The + or − sign after an oxygen atom designation indicates a position above or below the mirror planes cutting the *a* axis at $x=0$ and $x=0{\cdot}5$. The remaining four $O–H_2O–O$ bonds of subcell I can be derived from the Table by the symmetry transformation $P1c1$ $(x, -y, z+0{\cdot}5)$. The atomic arrangement of subcell I is repeated in subcell II. The atomic arrangements of subcell III and IV can be derived from the Table by interchanging the + and − sign of the oxygen atoms and their *x* coordinates.

Atom designation		*x*	*y*	*z*
H_2O	O(2)−	0·5−0·051	0·095	0·705
		0·280	0·187	0·514
	O(5)−	0·5−0·031	0·254	0·297
H_2O	O(4)+	0·5+0·060	0·010	0·409
		0·720	0·187	0·514
	O(7)+	0·5+0·041	0·378	0·505
H_2O	O(2)+	+0·051	0·595	0·705
		0·220	0·687	0·514
	O(5)+	+0·031	0·754	0·297
H_2O	O(4)−	−0·060	0·510	0·409
		0·780	0·687	0·514
	O(7)−	−0·041	0·878	0·505

8. Infrared investigation

The superstructure model is derived only from the average structure determination and from the features of the satellite diffraction pattern, but the intensities of the satellite reflexions are not considered. Therefore infrared absorption was used to check the model.

The following O···H–O bond lengths were obtained from the average and superstructure (see Table 2):

	Average structure	Superstructure
H_2O–O(2)	2·87 Å	2·66 Å
H_2O–O(7)	2·87	2·70
H_2O–O(4)	2·95	2·70
H_2O–O(5)	2·98	2·85
Mean	2·92	2·73

The infrared absorption spectrum is shown in Fig. 12. The O···H–O stretching absorption at 3250 cm^{-1} corresponds to an O···H–O distance of 2·78 Å (Hamilton & Ibers, 1968). This spectroscopic result agrees better with the superstructure bond distances than with those of the average structure.

Table 6. C_2O_4 *molecules of the superstructure*

The coordinates of the C_2O_4 groups correspond to the atomic arrangements of the C_2O_4 molecules in subcells I and II of Fig. 6(*b*). The coordinates are related to the axes of the subcell. The coordinates of the non-split atoms C(1)–C(4) and O(1), O(3), O(6) and O(8) are taken from Table 1 of Part I, and those of the split oxygens O(2), O(4), O(5) and O(7) are taken from Table 1 of this paper. A + or − sign after an oxygen atom designation indicates a position above or below the mirror planes cutting the *a* axis at $x=0$ and $x=0{\cdot}5$. The arrangements of the C_2O_4 molecules of subcells III and IV can be derived from the coordinates of this Table by interchanging the + and − signs of the oxygens. The coordinates of the remaining four C_2O_4 molecules of each subcell are generated by the symmetry transformation $P1c1$ $(x, -y, 0{\cdot}5+z)$.

Atom designation	*x*	*y*	*z*
First C_2O_4 molecule			
O(1)	0·0	0·246	0·305
O(2)+	+0·051	0·405	0·205
C(1)	0·0	0·348	0·297
C(2)	0·0	0·413	0·423
C(3)	0·0	0·357	0·524
O(4)−	−0·060	0·510	0·409
Second C_2O_4 molecule			
O(5)−	0·5−0·031	0·254	0·297
O(6)	0·5	0·406	0·181
C(3)	0·5	0·355	0·281
C(4)	0·5	0·428	0·404
O(7)+	0·5+0·041	0·378	0·505
O(8)	0·5	0·529	0·388
Third C_2O_4 molecule			
O(1)	0·5	0·746	0·305
O(2)−	0·5−0·051	0·905	0·205
C(1)	0·5	0·848	0·297
C(2)	0·5	0·913	0·423
O(3)	0·5	0·857	0·524
O(4)+	0·5+0·060	0·010	0·409
Fourth C_2O_4 molecule			
O(5)+	+0·031	0·754	0·297
O(6)	0·0	0·906	0·181
C(3)	0·0	0·855	0·281
C(4)	0·0	0·928	0·404
O(7)−	−0·041	0·878	0·505
O(8)	0·0	0·029	0·388

9. Degree of simplification

The superstructure model of Fig. 10(*b*) is not in full agreement with the average structure and with the satellite diffraction pattern.

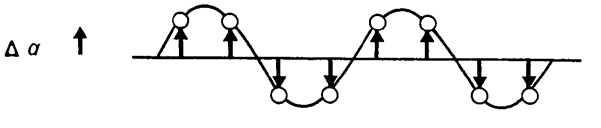

Fig. 11. Distortion wave of the proposed superstructure model.

Fig. 2(*b*) shows the thermal vibrational ellipsoids of the C_2O_4 groups with split atoms. The largest thermal axes for the split oxygens are sometimes larger than for the non-split oxygens. This is probably caused by further splitting and means the oxygen split positions are again only average positions. On following the directions of the largest axes of the split oxygens in Fig. 2(*b*) it appears that these oxygens occupy positions on a circle which has its centre at the C atoms, to which the split oxygens are bonded. The occupation possibility is different at different positions. It probably reaches a maximum at and nearly at the split positions calculated by the average structure determination.

b(super) = 4*b*(sub) holds for the superstructure model of Fig. 10(*b*). However, for the diffraction pattern of the satellite reflexions $n = 4{\cdot}7$ (§ 4). Furthermore, the diffraction photographs (*cf.* Fig. 5) show that the satellite reflexions are diffuse. The direction of diffuseness is parallel to **b***. It follows that $n = 4{\cdot}7$ is only the mean of different values and that the long-range order is not very well developed. The best formulation for the main features of the superstructure is therefore as follows.

The arrangement of O···H–O bonds is close to the arrangement shown in subcells I and II of Fig. 10(*b*) or close to those of subcells III and IV. In the direction of **b** one of these two arrangements is present in two to three subcells, then it changes to the alternative arrangement.

10. Discussion of average and superstructure

10.1. C_2O_4 *ions*

Average and superstructures contain two symmetry-independent C_2O_4 ions. In the average structure all atoms of the C_2O_4 groups occupy the special positions 4(*b*); this means that they lie in mirror planes, and the C_2O_4 ions are thus planar [Figs. 1(*b*), 2(*a*)]. The C_2O_4 groups are no longer planar when the split atoms are considered [Fig. 2(*b*)]. It is not possible to determine the real arrangement of atoms in a C_2O_4 ion from the average structure because each molecule contains two split-oxygen positions, which leads to four different combinations of oxygen arrangements in each C_2O_4 ion.

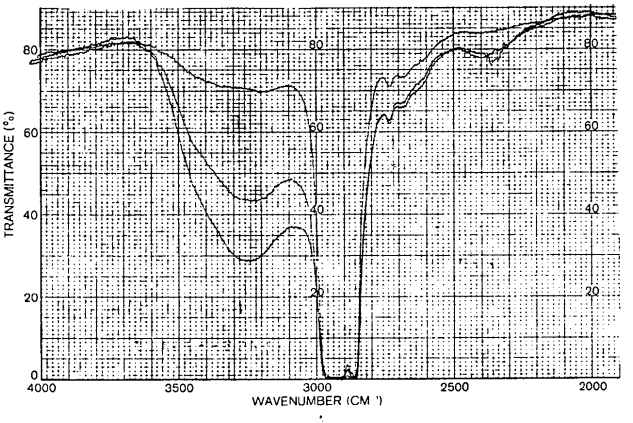

Fig. 12. Infrared absorption diagram of $K_2Mn(C_2O_4)_2.2H_2O$ at various concentrations (Nujol film technique). Absorption at 3250 cm^{-1} corresponds to H_2O absorption and that at 2900 cm^{-1} to Nujol absorption.

The true arrangement of the C_2O_4 ions as determined by the superstructure is shown in Fig. 2(*c*) and listed in Table 6. The CO_2 groups of the C_2O_4 ions are now twisted by 24 and 14° (Table 7). The corresponding C–C distances are 1·55 and 1·58 Å (Table 2). Comparable values of 27° and 1·569 (8) Å were reported for ammonium oxalate monohydrate (Robertson, 1965). From the superstructure investigation it follows that the split oxygens form C–O and O···H–O bonds, whereas the non-split oxygens form only C–O bonds (Table 2, additional oxygen bonds to Mn and K ions are described in §§ 3 and 10·2). The mean C–O distances in the superstructure are 1·267 (9) Å for the split oxygens and 1·248 (8) Å for the non-split oxygens. The differences of 0·019 (12) Å may be considered as significant: the C–O bonds are enlarged by formation of O···H–O bonds.

Table 7. *Twist of the* C_2O_4 *molecules in the superstructure*

First and third C_2O_4 molecules of Table 6	
Angle between the planes O(1)–C(1)–O(2) and O(3)–C(2)–O(4)	22·2°
Angle between the line C(1)–C(2) and a perpendicular line on the plane O(1)–C(1)–O(2)	69·5
Angle between the line C(1)–C(2) and a perpendicular line on the plane O(3)–C(2)–O(4)	66·3
Twist of the C_2O_4 molecule defined as the angle between the planes given by the line C(1)–C(2) and the perpendicular lines on the planes O(1)–C(1)–O(2) and O(3)–C(2)–O(4)	23·8
Second and fourth C_2O_4 molecules of Table 6	
Angle between the planes O(5)–C(3)–O(6) and O(7)–C(4)–O(8)	14·1
Angle between the line C(3)–C(4) and the perpendicular line on the plane O(5)–C(3)–O(6)	77·6
Angle between the line C(3)–C(4) and the perpendicular line on the plane O(7)–C(4)–O(8)	74·1
Twist of the C_2O_4 molecules defined as the angle between the planes given by the line C(3)–C(4) and the perpendicular lines on the planes O(5)–C(3)–O(6) and O(7)–C(4)–O(8)	14·1

The bond angles O–C–O range from 127 to 130° in the average structure and from 126 to 127° in the superstructure. The bond angles O–C–C range from 113 to 117° in the average structure and from 112 to 116° in the superstructure.

10.2. H_2O *molecules*, Mn *and* K *ions*

O–H_2O–O bonds are discussed in §§ 7 and 8.

The coordinating atoms of the Mn atoms are not influenced by the superstructure. The mean distances are Mn–O 2·20 Å, and Mn–H_2O 2·17 Å.

Only one coordination exists for the K atoms in the average structure, but two slightly different coordinations exist in the superstructure. The K–O distances range from 2·76 to 3·45 Å with a mean of about 2·8 Å.

APPENDIX

Calculation of satellite reflexion intensities

In the following it is assumed that the special positions 4(*a*) of space group $Cmc2_1$ are influenced by the same type of distortion waves, but that these distortion waves have phase shifts relative to each other. The phase relations between the distortion waves in the investigated crystals are known, if the main features of the observed and calculated satellite reflexion pattern agree.

The following assumptions are made:

(1) In the average structure atoms of scattering power f occupy the special positions 4(*a*):

$$\begin{array}{lllll}(a) & 0, & y, & z\\ (b) & \frac{1}{2},\frac{1}{2}+y, & & z\\ (c) & 0, & -y,\frac{1}{2}+z\\ (d) & \frac{1}{2},\frac{1}{2}-y,\frac{1}{2}+z\,. & & & (1)\end{array}$$

(2) The orthorhombic subcells are characterized by the axes *a*, *b* and *c*. The crystal volume is $V=Ma\,Nb\,Oc$. The running indexes in the following summations are *m*, *n*, *o*.

(3) $G(h)$, $G(k)$ and $G(l)$ are the Laue factors. The derivation of $G(h)$ is shown in the following:

$$\begin{aligned}G(ah)&=\sum_{m=0}^{M-1} f\exp 2\pi iHa(x+m)\\ &=f\exp 2\pi iHax\,\frac{1-\exp 2\pi iHam}{1-\exp 2\pi iHa}\\ &=f\exp 2\pi iHax\exp 2\pi i(M-1)Ha\\ &\quad\times\frac{\sin\pi NHa}{\sin\pi Ha}\end{aligned}$$

$G(ah)G^*(ah)=f^2M^2$ for $h=aH=$integer.

Similar relations hold for $G(k)$ and $G(l)$.

(4) A superstructure is generated by sinusoidal distortion waves. Their directions are parallel to **b** with the relation

$$b(\text{super})=pb(\text{sub})\quad p>2\,.$$

Only the x coordinates are influenced by the distortion wave according to

$$x=A\sin 2\pi\left(\frac{n}{p}\right)\quad A\ll 1\,. \qquad (2)$$

From (1) and (2) the coordinates within the supercell can be written as

$$\begin{array}{ll}(a) & A\sin 2\pi\left(\frac{n}{p}\right),y,z\\ (b) & \frac{1}{2}+A\sin 2\pi\left(\frac{n}{p}+q\right),\frac{1}{2}+y,z\\ (c) & A\sin 2\pi\left(\frac{n}{p}+r\right),\bar{y},\frac{1}{2}+z\\ (d) & \frac{1}{2}+A\sin 2\pi\left(\frac{n}{p}+s\right),\frac{1}{2}-y,\frac{1}{2}+z\end{array} \qquad (3)$$

$0<q,r,s<1$ (coefficients of the phase shift).

These relations mean: The positions (*a*)–(*d*) of (1) are influenced by the same distortion wave, but the four distortion waves may have phase shifts relative to each other. Compared with position (*a*) these phase shifts are $2\pi q$ for position (*b*), $2\pi r$ for position (*c*), and $2\pi s$ for position (*d*).

The wave diffracted by the superstructure is designated as $F(hkl)$, where h,k,l should be considered *at the moment* as variable coordinates of reciprocal space, which change into fixed values during the following calculation given by the argument of the corresponding Laue factors.

$$\begin{aligned}F(hkl)=\sum_{m,n,o=0}^{M-1,N-1,O-1} & f\{\exp 2\pi i[hA\sin 2\pi n/p+hm\\ &+kn+lz+lo]\\ &+\exp 2\pi i[h/2+hA\sin 2\pi(n/p+q)+hm+k/2\\ &+ky+kn+lz+lo]\\ &+\exp 2\pi i[hA\sin 2\pi(n/p+r)+hm-ky+kn\\ &+l/2+lz+lo]\\ &+\exp 2\pi i[h/2+hA\sin 2\pi(n/p+s)+hm+k/2\\ &+ky+kn+l/2+lz+lo]\}\\ &=fG(h)G(l)\sum_{n=0}^{N-1}\exp 2\pi ikn\\ &\times\{\exp 2\pi i[ky+lz]\sum_{n=0}^{N-1}\exp 2\pi i[hA\sin 2\pi n/p]\\ &+\exp 2\pi i[h/2+k/2+ky+lz]\\ &\times\sum_{n=0}^{N-1}\exp 2\pi i[hA\sin 2\pi(n/p+q)]\\ &+\exp 2\pi i[l/2-ky+lz]\\ &\times\sum_{n=0}^{N-1}\exp 2\pi i[hA\sin 2\pi(n/p+r)]\\ &+\exp 2\pi i[h/2+k/2+l/2-ky+lz]\\ &\times\sum_{n=0}^{N-1}\exp 2\pi i[hA\sin 2\pi(n/p+s)]\}\,. \qquad (4)\end{aligned}$$

(4) contains exponential functions which have a sine function in their argument. These exponential functions can be transformed by the relation

$$\exp 2\pi i[hA \sin 2\pi n/p] = \sum_{m=-\infty}^{\infty} J_m(2\pi hA) \times \exp[2\pi imn/p]. \quad (5)$$

Using only the Bessel functions with $m=0$ and $m=\pm 1$ (5) reduces to (6)

$$\exp 2\pi i[hA \sin 2\pi n/p] = J_0(2\pi hA) + J_1(2\pi hA) \exp 2\pi i[n/p] + J_{-1}(2\pi hA) \exp 2\pi i[-n/p]. \quad (6)$$

From (6), equation (4) can be transformed into (7):

$$\begin{aligned} F_{hkl} = f\,.\, & G(h)G(l) \\ & \times [G(k)J_0(2\pi hA)\{\exp 2\pi i[ky+lz] + \exp 2\pi i[h/2 \\ & + k/2 + ky + lz] + \exp 2\pi i[l/2 - ky + lz] \\ & + \exp 2\pi i[h/2 + k/2 + l/2 - ky + lz]\} \\ & + G(k+1/p)J_1(2\pi hA)\{\exp 2\pi i[ky+lz] \\ & + \exp 2\pi i[h/2 + k/2 + ky + lz] \exp 2\pi iq \\ & + \exp 2\pi i[l/2 - ky + lz] \exp 2\pi ir \\ & + \exp 2\pi i[h/2 + k/2 + l/2 - ky + lz] \exp 2\pi is\} \\ & + G(k-1/p)J_{-1}(2\pi hA)\{\exp 2\pi i[ky+lz] \\ & + \exp 2\pi i[h/2 + k/2 + ky + lz] \exp 2\pi i[-q] \\ & + \exp 2\pi i[l/2 - ky + lz] \exp 2\pi i[-r] \\ & + \exp 2\pi i[h/2 + k/2 + l/2 - ky + lz] \exp 2\pi i[-s]\}]. \end{aligned} \quad (7)$$

For the diffracted intensities

$$I_{hkl} = F_{hkl}\, F^*_{hkl}$$

I_{hkl} is observable if the products of the Laue factors $GG^* \neq 0$. Therefore the main reflexions are only observable if h,k,l = integer. The satellite reflexions are only observable if h = integer, $k' = k \pm 1/p$ with k = integer, l = integer.

Instead of considering the expressions for the intensities of the main and satellite reflexions, it is more convenient to consider only the expressions for the corresponding F values:

Main reflexions:

$$\begin{aligned} F_{hkl} = f & G(h)G(k)G(l)J_0(2\pi hA) \\ & \times \{\exp 2\pi i[ky+lz][1+(-1)^{h+k}] \\ & + \exp 2\pi i[l/2 - ky + lz][1+(-1)^{h+k}]\}. \end{aligned} \quad (8)$$

Satellite reflexions:

$$\begin{aligned} F_{hk'l} = f & G(h)G(k')G(l)J_1(2\pi hA) \\ & \times \{\exp 2\pi i[k'y+lz][1+(-1)^{h+k'} \exp 2\pi iq] \\ & + \exp 2\pi i[l/2 - k'y + lz][\exp 2\pi ir + (-1)^{h+k'} \\ & \times \exp 2\pi is]\}. \end{aligned} \quad (9)$$

$F_{hk''l}$ can be derived from (9) by replacing (k', q, r, s) by $(k'', -q, -r, -s)$.

Discussion

For the main reflexions from (8)

if $h+k$ = odd, then $F_{hkl} = 0$

if $h+k$ = even, then

$$F_{hkl} = fG(h)G(k)G(l)J_0(2\pi hA)\{2 \exp 2\pi i[ky+lz] + 2 \exp 2\pi i[l/2 - ky + lz]\}.$$

$$I_{hkl} = F_{hkl}\, F^*_{hkl} = f^2M^2N^2O^2J_0^2(2\pi hA) \times \{8 + 8 \cos(l/2 - 2ky)\}. \quad (10)$$

This means: main reflexions are present at the places expected from the space-group symmetry of the average structure, but the diffracted intensity is given by (10), which contains the term $J_0^2(2\pi hA)$, by which the diffracted intensity is weakened with increasing h. The consequence is that the atoms which provide intensity for the satellite reflexions have a pseudo-anisotropic thermal vibrational ellipsoid with an unusually large principal thermal axis parallel to **a**, if the structure investigations are based on the main reflexions only.

For the satellite reflexions from (9)

if $h+k'$ = even, then

$$\begin{aligned} F_{hk'l} = f & G(h)G(k')G(l)J_1(2\pi hA) \\ & \times \{\exp 2\pi i[k'y+lz][1+\exp 2\pi iq] \\ & + \exp 2\pi i[l/2 - k'y + lz][\exp 2\pi ir + \exp 2\pi is]\}. \end{aligned} \quad (11)$$

if $h+k'$ = odd, then

$$\begin{aligned} F_{hk'l} = f & G(h)G(k')G(l)J_1(2\pi hA) \\ & \times \{\exp 2\pi i[k'y+lz][1-\exp 2\pi iq] \\ & + \exp 2\pi i[l/2 - k'y + lz][\exp 2\pi ir - \exp 2\pi is]\}. \end{aligned} \quad (12)$$

A similar result can be derived for $F_{hk''l}$.

As described in § 4, the satellite reflexions appear only around the 'extinct' main reflexions with $h+k$ = odd. It follows that (11) has to be equal to zero This is only possible if $q = \frac{1}{2}$ and $s = r + \frac{1}{2}$. With these values, (12) transforms into (13):

$$\begin{aligned} F_{hk'l} = f & G(h)G(k')G(l)J_1(2\pi hA) \\ & \times \{2 \exp 2\pi i[k'y+lz] + 2 \exp 2\pi i[l/2 - k'y + lz] \\ & \times \exp 2\pi ir\}. \end{aligned} \quad (13)$$

Fig. 5(*b*) shows that the satellite reflexions, which appear around the 'extinct' main reflexions with $h=1$, $k=0$, l = odd, have very weak intensities. Let us assume that these satellite reflexions are exactly zero. Then (13) has to be zero, if $k'=0$ and l = odd. This is only possible, if $r=0$. The same results can be derived for $F_{hk''l}$.

In this way the values of q,r,s are determined: $q=\frac{1}{2}$, $r=0, s=\frac{1}{2}$. Putting these values for q,r,s into (3) gives

$$\begin{aligned}
&(a)\quad A\sin 2\pi\left(\frac{n}{p}\right), y, z\\
&(b)\quad \tfrac{1}{2}-A\sin 2\pi\left(\frac{n}{p}\right), \tfrac{1}{2}+y, z\\
&(c)\quad A\sin 2\pi\left(\frac{n}{p}\right), \bar{y}, \tfrac{1}{2}+z\\
&(d)\quad \tfrac{1}{2}-A\sin 2\pi\left(\frac{n}{p}\right), \tfrac{1}{2}-y, \tfrac{1}{2}+z\,. \qquad (14)
\end{aligned}$$

By this atomic arrangement all symmetry elements of the space group of the subcell $Cmc2_1$ are destroyed except the c glide plane. The remaining symmetry of the subcells of a supercell is therefore $P1c1$.

I am indebted to Professor H. Saalfeld, Dr H. Siems and Dr Wedde of the Mineralogisch-Petrographisches Institut, Universität Hamburg, for their helpful discussion, to Dr Siems for his calculation of the values of Table 7, and to Dr Wedde for his careful inspection of the manuscript. The single-crystal diffractometer used for the measurement was made available by the Owens Illinois Co., Toledo, Ohio, USA, who also supported the work financially.

References

DEHLINGER, U. (1927). *Z. Kristallogr.* **65**, 615–631.
HAMILTON, W. C. & IBERS, J. A. (1968). *Hydrogen Bonding in Solids*, p. 87. New York: Benjamin.
International Tables for X-ray Crystallography (1962). Vol. III, pp. 201–207. Birmingham: Kynoch Press.
KOREKAWA, M. (1967). *Theorie der Satellitenreflexe*. Habilitationsschrift, Universität München.
MATTHIES, H. & SCHULZ, H. (1968). *Naturwissenschaften*, **55**, 342.
ROBERTSON, J. H. (1965). *Acta Cryst.* **18**, 410–417.
STEWART, J. M., KRUGER, G. J., AMMON, H. L., DICKINSON, G. & HALL, S. R. (1972). The X-RAY System of Crystallographic Programs. Technical Report TR-192, Computer Science Centre, Univ. of Maryland.
WILSON, A. J. C. (1962). *X-ray Optics*, pp. 113–118. London: Methuen.

Acta Cryst. (1974). B**30**, 1332

The Crystal Structure and Molecular Conformation of 3,7-Dichlorophenoselenazine

BY F. BERNIER, A. CONDE AND R. MÁRQUEZ

Departamento de Optica, Sección de Física del Departamento de Investigaciones Físicas y Químicas (Centro Coordinado del CSIC), Universidad de Sevilla, Spain

(*Received* 2 *January* 1974; *accepted* 11 *January* 1974)

The crystal structure of $SeCl_2NC_{12}H_7$ has been solved by Patterson and Fourier methods and refined to an R of 7·5% by full-matrix least-squares methods. The unit cell is orthorhombic, with $a=7{\cdot}995$ (3), $b=23{\cdot}808$ (1), $c=6{\cdot}028$ (2) Å and four molecules in the cell. The space group is *Pnma*. The structure contains layers of molecules centred on the mirror planes at $b/4$ and $3b/4$.

Introduction

The structural analyses of several phenazine derivatives have been carried out, especially of compounds including the phenothiazine heterocycle, but until now there has been no information about the structural details of the analogous selenium compounds. The structure determination of 3,7-dichlorophenoselenazine was undertaken as part of a series of structural analyses of organoselenium compounds. The determination of the Se–C bond lengths and the C–Se–C bond angles will provide information on the bonding characteristics of the selenium atom.

Experimental

Crystals of 3,7-dichlorophenoselenazine were supplied by Professor Pino of the Departamento de Química Analítica of this University. Single crystals used in this work were obtained by slow evaporation at room temperature from solutions in chloroform. The crystals are yellow-green and have laminar shape, the b axis being perpendicular to the plate. In spite of considerable effort it was not possible to grow crystals much wider than 0·1 mm. The density was determined by the flotation equilibrium method in an aqueous solution of zinc bromide.

Preliminary unit-cell dimensions were determined from rotation and Weissenberg photographs. The diagrams indicated orthorhombic symmetry and the systematic absences were consistent with either *Pnma* or $Pn2_1a$ space groups. Accurate cell parameters were measured with Mo $K\alpha$ radiation on a Philips PW 1100 four-circle diffractometer. The crystal data are summarized below.